Eur. Phys. J. B **18**, 535–540 (2000)

THE EUROPEAN PHYSICAL JOURNAL B

EDP Sciences

Optical transmittance spectroscopy of concentric-shell fullerenes layers produced by carbon ion implantation

Th. Cabioc'h[1,a], S. Camelio[1], L. Henrard[2], and Ph. Lambin[2]

[1] Laboratoire de Métallurgie Physique[b], Université de Poitiers, SP2MI, Téléport 2, boulevard Pierre et Marie Curie, BP 30179, 86962 Futuroscope Cedex, France
[2] Département de Physique, Facultés Universitaires Notre-Dame de la Paix, 61 Rue de Bruxelles, 5000 Namur, Belgium

Received 13 July 2000

Abstract. Concentric-shell fullerenes, also called carbon onions, produced by carbon ion implantation into silver thin films, and subsequently deposited on a silica substrate, were studied by optical transmission spectroscopy in the wavelength range 0.2 – 1.2 μm. In this interval, the strongest absorption is due to the π-plasmon of sp^2-like carbon. The position of the plasmon absorption band clearly evolved from 265 nm at low fluence to 230 nm at high implantation fluences. A simulation of the optical spectra based on dielectric models of the concentric-shell fullerenes layer allowed us to identify the first peak as due to disordered graphite and the latter to the carbon onions. The concentration of residual graphite and the filling fraction of the carbon onions produced at high fluences could be estimated by fitting the optical spectra with computed transmittance curves.

PACS. 78.66.Tr Fullerenes and related materials – 68.55.-a Thin film structure and morphology

1 Introduction

Since their discovery [1], carbon onions have attracted much attention because of their structure which presents a fascinating degree of symmetry [2]. Furthermore, some of their physical properties could be considered as attractive [3]. For instance, these carbon nanostructures are potentially good solid lubricants as it is the case for WS_2 nanoparticles having an onion-like structure [4]. But the main point of interest, as far as this new carbon nanostructure is concerned, remains their possible presence in the interstellar dust where, more specifically, carbon onions could contribute to the strong absorption band centered at 217.5 nm [5–8]. Theoretical investigations of the optical properties of carbon onions have been undertaken [9–12] but the minute quantity of available material has prevented direct optical measurement. A pioneer experimental work has been performed by de Heer and Ugarte [6] who measured the optical absorption in the UV-visible range of onion-like carbon nanostructures produced by thermal annealing of carbon black. Nevertheless these optical results, the main features of which have been reproduced [13] within the dielectric model [9,10], do not fit the astrophysical data. The main reasons are that the carbon onions were poorly formed, strongly linked together, and the nanostructures were diluted into water.

New results were obtained recently by Wada *et al.* [14] on carbon onions formed on cold parts of a CVD apparatus. These data came closer to the interstellar dust spectra since an absorption peak centered at 220 nm was obtained. Nevertheless, the redshift to 240 nm of the absorption peak which appeared after subsequent annealing of the material remains poorly understood. Such a redshift (from 215 nm to 250 nm) has also been observed by Blanco *et al.* [15] on freshly formed and annealed amorphous carbon produced in hydrogen-rich and hydrogen-poor atmosphere. But the authors of both publication did not clearly establish a correlation between the evolution of the structure of the carbon material and that of the optical data.

In most instances, the lack of macroscopic quantities of carbon onions has limited the experimental studies devoted to the structure and properties of these novels carbon nanostructures. This lack has been evaded in part by the use of local electronic probe techniques. For instance, High Resolution Transmission Electron Microscopy (HRTEM) has been widely used to discuss the structure [16–19] of carbon onions whereas Scanning Transmission Electron Microscopy (STEM) have confirmed the excitation of surface plasmon. It is interesting to note that the dieletric theory adapted to the special anisotropy of onion-like molecules has proven to correctly reproduce these last experimental data [20,21].

A few methods able to produce enough carbon onion material to study some of the carbon onions properties

[a] e-mail: Thierry.Cabioch@lmp.univ-poitiers.fr
[b] UMR 6630 CNRS

have became available today. For instance, thermal annealing of diamond nanoparticles [22] or carbon black [6] are powerful for synthesizing numerous carbon onions. Nevertheless, in both cases, the carbon nanostructures are often polyhedral and clumped. In addition to these annealing experiments, an original method, based on ion-implantation, has been developed to achieve the synthesis of controlled-sized spherical carbon onions [23]. This last method consists in high-fluence carbon ion-implantation into silver substrates held at elevated temperature ($> 400\,^{\circ}$C). Nevertheless, due to the presence of silver substrate, the study of the properties of carbon onions so synthesized is difficult. This is the main reason why a three-step technique devoted to the synthesis of pure carbon onion layers deposited onto silica substrate was recently developed [24]. The silica being transparent in a large wavelength range, the study of the transmittance properties of the carbon onion layers becomes feasible.

In this contribution we present optical transmittance of carbon onion layers deposited onto silica substrates and produced by this implantation technique (Sect. 2), the results being analyzed on the basis of theoretical simulations using the dielectric model (Sect. 3). Our results show two major contributions to the absorption spectra at 220 nm and 265 nm. In Section 4, we analyse the implication of the microstructure of the carbon onion on the optical spectra and we attributed the 220 nm and 265 nm features to carbon onions and residual misoriented carbon sp^2 microscopic units, respectively.

2 Experimental results

Carbon onions have been produced by high fluence 120 keV carbon ion implantation into silver thin films, 400 nm thick, deposited by ion-beam sputtering onto silica substrates (Suprasil from Heraeus). We systematically varied the fluence from 0.5 to 3×10^{17} ions/cm^2 to obtain different average sizes for the carbon onions. In one case, the current density was also modified (6 to 15 μA/cm^2) to determine the influence of this parameter on the optical properties of the carbon layer. After these implantation experiments, carbon onions are distributed inside the silver thin film. The top of some spherical carbon onions can simply be observed by Atomic Force Microscopy (AFM) when the implanted fluence exceeded 5×10^{16} ions/cm^2. It can be outlined that no delamination of the silver film prior or after the implantation was observed by optical microscopy or by AFM. Pure carbon onion layers were obtained after removal of the silver component by using a thermal annealing in vacuum (850 °C, 10^{-5} Pa). Carbon onions very poorly adherent to the silica were then obtained. They were collected onto copper grids for high-resolution transmission electron microscopy (HRTEM) observations. These were performed in a JEOL 3010 apparatus working at 300 kV. The optical transmittance of the carbon layers has been deduced from measurements performed with a spectrophotometer in transmission mode in the wavelength range 0.2 – 1.2 μm. In this interval, the silica substrates are almost transparent. The apparatus was operated at normal incidence with a Xe lamp (75 W) and with a double monochromator (grating and prism).

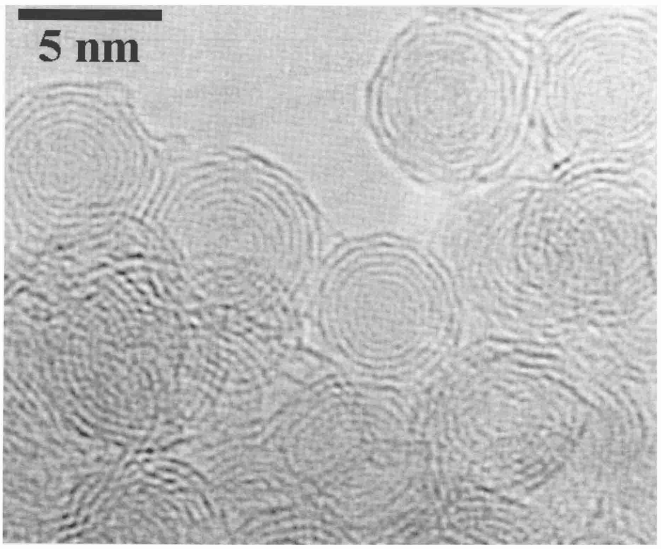

Fig. 1. HRTEM micrography of carbon onions synthesized by 120 keV carbon ion-implantation (fluence: 10^{17} ions/cm^2, temperature: 500 °C, current density: 6 μA/cm^2) in a silver thin film and after a thermal annealing at 850°C in vacuum.

Figure 1 shows a typical HRTEM micrography of carbon onions synthesized after an implantation of 2×10^{17} cm^{-2} carbon ions in a silver thin film, 300 nm thick, at 500 °C. Almost perfectly spherical carbon onions were identified. Circular dark contrasts corresponding to graphite layers separated by a distance of 0.34 nm were obtained. The carbon onions constitute almost the entire part of the matter that could be characterized during the HRTEM inspection of the samples. Nevertheless, some carbon residues, poorly crystallized, were observed occasionally between the carbon onions. More especially, we observed that the quantity of these carbon residues decreased as soon as the implanted carbon fluence increased. In addition, as described elsewhere [24], the average diameter of the carbon onions increased with increasing fluence. Typically, the mean diameter of carbon onions increased progressively from approximatively 4 to 8 nm when the fluence was varied from 5×10^1 ions/cm^2 to 3×10^{17} ions/cm^2 with an implantation temperature being fixed at 500 °C. It is important to note that a micrography as shown in Figure 1 allows one to discuss the structure of the onions themselves, but it does not give a clear view of the microstructure of the carbon layers which is just deposited onto the silica substrates and optically characterized. The carbon onions characterized by HRTEM are present on a copper TEM grid in a powder form which was obtained by a mechanical scratching of the carbon onion layer. Besides, the carbon onions are not homogeneously dispersed on the copper TEM grids and it explains why a clumping of carbon onions was observed. Individual carbon onions as those shown in Figure 1 were thus only resolved on the borders of the agglomerates. It is then obviously

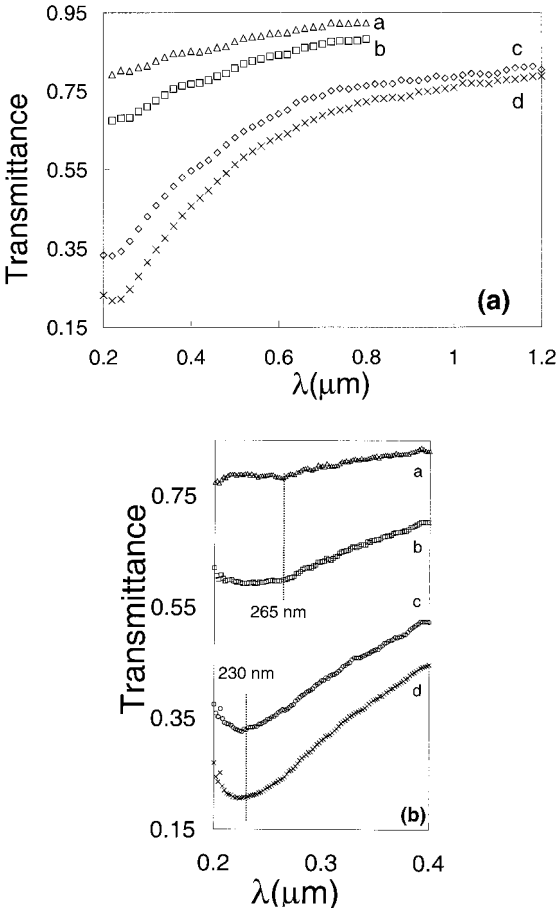

Fig. 2. Optical transmittance of carbon-onion layers obtained by the implantation of 120 keV carbon ions into Ag held at 500 °C for various fluences (a: 5×10^{16}, b: 10^{17}, c: 2×10^{17}, d: 3×10^{17} ions/cm^2). Pannels (a) and (b) correspond to two spectral ranges with different resolutions.

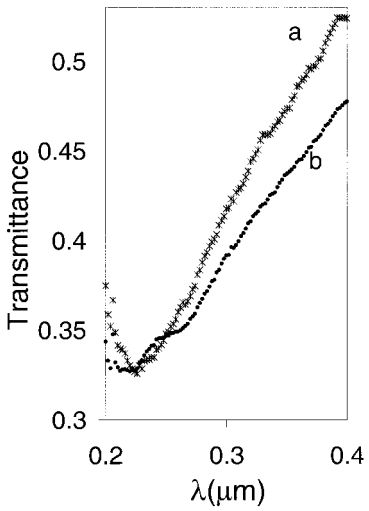

Fig. 3. Optical transmittance of carbon-onion layers obtained for the implanted fluence of 2×10^{17} ions/cm^2 with two current densities of the carbon ion beam (a: 15, b: 6 μA/cm^2).

impossible to discuss the distribution of the carbon onions in the film itself and the quantity of carbon which precipitate into the silver layer in another form (carbon residues) than carbon onions. In parallel to these TEM characterizations, Electron Energy Loss Spectroscopy spectra have also been obtained on carbon onions powder so formed. They indicate that all the silver component was evaporated after the silver process. Nevertheless, some impurities could be observed: very few metallic (Fe, Au, ...) nanoparticles could so be characterized. The presence of such impurities was simply attributed to the sputtering of the walls of the vacuum chamber during the deposition process. It must be outlined that a contribution of these metallic nanoparticles to the optical data described below was not detected.

The optical transmittance of different carbon onion layers, as a function of the implanted fluence, is presented in Figure 2. The fact that the transmittance decreases by increasing fluence can simply be explained by the increase of the average thickness of the carbon layer. Indeed, by assuming that the carbon onions and the carbon residues have a density close to that of graphite (2.25 g/cm^3), it is possible to estimate an equivalent thickness (in nm) of a deposited dense carbon layer from the relation $\Phi/11.3 \times 10^{15}$ where Φ is the implanted fluence (in cm^{-2}). For the different fluences presented in the Figure 2, the equivalent thickness of the carbon layers so varied from about 4 to 26 nm. The second important remark that can be made from this figure concerns the evolution of the absorption peak position. Indeed, if only a small peak centered around 0.265 μm can be observed for the lowest fluences (0.5 and 1×10^{17} ions/cm^2), a second peak close to 0.230 μm comes out for the highest fluences (2 and 3×10^{17} ions/cm^2).

Figure 3 displays the optical transmittance of carbon onion layers obtained for a same implanted fluence, but with different current densities of the carbon ion beam (6 and 15 μA/cm^2). If a peak centered around 0.22– 0.23 μm is identified in both cases, a shoulder at a position close to 0.265 μm can clearly be observed for the lowest current density. Such a difference in the shape of the transmittance curves clearly indicates the strong influence of the experimental implantation conditions on the optical properties of the onion layers. It is also worth mentioning that, during HRTEM observations, no significant modification of the carbon onion structure (shape, size) was noticed for a given fluence when the current density was varied.

3 Simulation

Further characterization of the onion films was obtained by comparing the experimental optical transmission curves with theoretical simulations. A continuous-medium dielectric approximation was used to describe the optical properties of the carbon onions [10]. The effective dielectric function of the onion layer was assumed to follow

the Clausius-Mossotti expression

$$\epsilon = \epsilon_{\rm e}\left(1 + \frac{f\alpha}{1 - f\alpha/3}\right) \tag{1}$$

where $\epsilon_{\rm e}$ is the dielectric function of the medium external to the onions, α is the dipolar polarisability of the onions in units of $\epsilon_0 V$, with V the onion volume, and f is the filling fraction. For plain onions (*i.e.* for a vanishing inner cavity radius), the dimensionless polarisability was computed by the equation [9]

$$\alpha = 3\frac{u\epsilon_{\parallel} - \epsilon_{\rm e}}{u\epsilon_{\parallel} + 2\epsilon_{\rm e}} \tag{2}$$

with

$$u = \left(\sqrt{1 + 8\epsilon_{\perp}/\epsilon_{\parallel}} - 1\right)/2 \ , \ {\rm Re}\ u > 0 \tag{3}$$

where $\epsilon_{\perp}$ and $\epsilon_{\parallel}$ are the principal components of the dielectric tensor of graphite in the directions perpendicular and parallel to the c-axis. In the non-retarded approximation used here, the polarisability per volume unit, α, does not depend on the diameter of the onions.

The Clausius-Mossotti equation applies strictly to point-like dipoles on a cubic crystal. For the case of dielectric spheres as considered here, corrections arise from multipole orders higher than two (the quadrupoles play no role since their summation on a cubic lattice vanishes) [25]. We did not attempt to include these corrections in the model since the assumption that the onions are located on a cubic lattice has probably more severe effects. In addition, the many uncertainties on the dielectric function of graphite, more especially for the out-of-plane component $\epsilon_{\parallel}$, constitute another source of error [26,27].

The HRTEM pictures indicate a small concentration of carbon residues in the voids between the onions. This residual carbon was introduced in the simulation of the transmittance spectra in the form of an effective medium with dielectric function equal to one third the trace of the dielectric tensor of graphite. This approximation corresponds to randomly-oriented microscopic units of graphite [28], which is justified by the fact that the carbon residues were partly graphitized by the annealing of the samples at 850 °C. Accordingly, the dielectric function of the medium external to the onions was described by

$$\epsilon_{\rm e} = (1 - c) + c(2\epsilon_{\perp} + \epsilon_{\parallel})/3 \tag{4}$$

where c is the volume concentration of the residual carbon in the voids.

The transmittance of the effective layer (effective thickness d) deposited on a thick silica substrate (refractive index $n_{\rm s}$), was computed with standard electromagnetism. The experimental transmittance, measured in normal incidence, were divided by the transmission coefficient of the clean substrate, $4n_{\rm s}/(1+n_{\rm s})^2$. At normal incidence, the transmission coefficient of the film so renormalized writes

$$t(\lambda) = \frac{(1 + n_{\rm s})^2}{\left|(1 + n_{\rm s})\cos(2\pi\sqrt{\epsilon}d/\lambda) - {\rm i}(\sqrt{\epsilon} + n_{\rm s}/\sqrt{\epsilon})\sin(2\pi\sqrt{\epsilon}d/\lambda)\right|^2}. \tag{5}$$

This formula was used for all the simulations. It is a generalization of the formulation found in standard textbooks [29] to the case were the media on both sides of the film are different. To first order in d/λ, it reduces to

$$t(\lambda) \approx 1 - \frac{4\pi d/\lambda}{1 + n_{\rm s}}\ {\rm Im}\ \epsilon. \tag{6}$$

In all the calculations, the dielectric principal components $\epsilon_{\parallel}$ and $\epsilon_{\perp}$ of graphite were taken from Draine and Lee's data [30]. In the measurements, the transmittance of the silica substrate varied between 0.92 and 0.96 within the wavelength interval explored. In the simulation, a constant index $n_{\rm s} = 1.65$ was used, which corresponds to the average value 0.94 of the substrate transmittance.

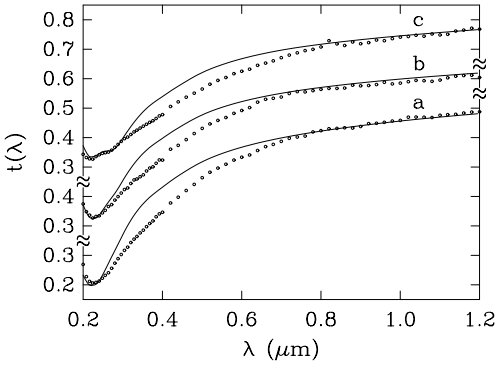

Fig. 4. Simulation of the transmittance of carbon onion layers (full curves) compared with experimental data (dots). The labels a, b, and c corresponds to the parameters listed in Table 1. The curves b and c were shifted vertically for clarity.

Three computed transmittance curves are shown in Figure 4, where the simulation is compared to experiment. The filling fraction of the onions was adjusted as follows. The imaginary part of the polarisability of an isolated carbon onion computed from equation 2 has a peak at $\lambda = 0.21\,\mu$m attributed to a collective electron transition from bounding to antibounding π states (π-plasmon). This peak of Im α corresponds to a maximum of the absorption cross section of the carbon onions and, therefore, to a minimum of the transmittance. Packing the carbon onions together shifts the transmittance minimum to the red [10]. With $f = 0.6$, the minimum takes place at the experimental value, $0.23\,\mu$m. Small deviations from this value were observed, depending on the fluence. Nevertheless, the same value $f = 0.6$ was used for all the curves of Figure 4. By comparison, the π-plasmon peak of the carbon onions was observed at 5.7 eV ($0.22\,\mu$m) in electron-energy-loss spectroscopy [21,23,31,32].

The effective thickness of the layer was estimated from the fluence. A fluence of $10^{17}\,{\rm cm}^{-2}$ corresponds

Table 1. Parameters used for the simulation of the transmittance spectra (d: film thickness, c: graphite concentration in the voids between carbon onions).

film	experimental conditions	d (nm)	c
a	3×10^{17} cm^{-2}, 15 μA/cm^2	40	0.03
b	2×10^{17} cm^{-2}, 15 μA/cm^2	28	0.04
c	2×10^{17} cm^{-2}, 6 μA/cm^2	28	0.075

to a deposition of a 8.8 nm dense carbon layer. The effective thickness of the carbon onion layer with filling fraction f is therefore of the order of $8.8/f$ nm. The thickness calculated from that expression was slightly readjusted so as to fit both the minimum of the transmission curve around $\lambda = 0.23\,\mu$m and the curve in the interval 1–1.2 μm. Finally, the concentration of graphitic residues in the voids was adjusted to the transmittance curves around $\lambda = 0.26\,\mu$m, where some of the experimental spectra have a shoulder. This concentration ranged from 3% for the sample (a) produced with a high current density to 7.5% for sample (c) obtained at low current.

The values of the parameters used in the simulation are listed in Table 1. If the agreement with the experimental data is fair, it is not perfect, more especially in the wavelength interval 0.3–0.7 μm. We did not attempt to improve the agreement any further, given the many uncertainties on the graphite dielectric data. Despite of these, the adjustment of the parameters gives a coherent picture of what the implanted layer is made from. This aspect is discussed in the next section.

4 Discussion

The optical spectra clearly show two absorption peaks at 0.265 and 0.23 μm. The first peak dominates the transmittance spectrum at low fluences. The intensity of the second peak increases with increasing implantation fluence and, eventually, dominates the spectrum. Both the microscopic analysis and the optical simulations indicate that this 0.23 μm absorption is due to the carbon onions packed together into the layer. Even at high fluences, a shoulder structure remains in the spectra at 0.265 μm, especially at low current density. This peak is attributed to a small fraction of residual graphitic material inside the voids between the carbon onions.

At low fluence, the quantity of the graphitic residues is sufficient to mask the spectral response of the carbon onions. This effect is illustrated by the transmittance curves of Figure 5 that were computed for increasing concentrations c of residual graphite in the voids. The thickness layer was kept fixed at 15 nm, corresponding to an implanted fluence of 10^{17} ions/cm^2. Already at $c = 0.08$, the peak at 0.265 μm acquires the same intensity as the one at 0.23 μm. With 10% of graphitic residues and above, the carbon onion signature is reduced to just a shoulder and progressively disappears. In the model, c denotes the concentration of graphitic residues in the voids. The actual proportion of residue with respect to the deposited carbon is $c(1-f)/[f + c(1-f)]$. With $f = 0.6$ and $c = 0.1$, this proportion is close to 6%. Such a low fraction of residual graphite can hardly be estimated by HRTEM due to the two-dimensionnal representation obtained by TEM but also because this carbon material presents very low amorphous-like contrasts as compared to the carbon onions which are always in Bragg diffraction conditions. The simulations presented here show that the optical response of the carbon onion layers are very sensitive to the presence of residual carbon. Besides, this high sensitivity made it possible to estimate that contamination, which otherwise would have been difficult to measure.

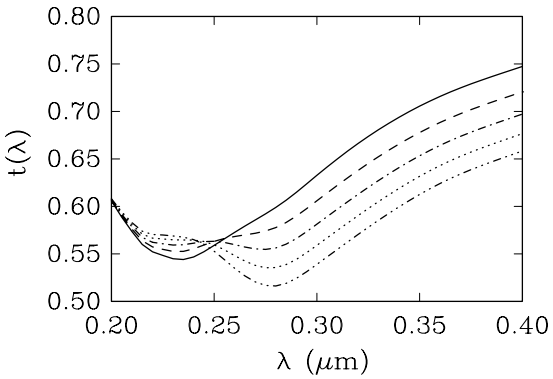

Fig. 5. Transmittance spectra computed for a 15 nm thick layer with increasing concentrations of carbon residues between the carbon onions: $c = 0.04$ (full curve), 0.06 (dashed curve), 0.08 (dot-dashed curve), 0.10 (dotted curve), and 0.12 (dot-dot-dashed curve). The carbon onion filling fraction was kept constant ($f = 0.6$).

This observation sheds some light on the growth mechanism of the different carbon phases formed during the implantation. It indicates that the carbon residues mainly form at the beginning of the implantation process. This is confirmed by independent HRTEM observations performed on *bulk* silver samples implanted with low C fluences (work in progress). After a fluence of approximatively 10^{17} ions/cm^2, the formation of carbon residues stops while the carbon onions continue growing. This explains why the relative proportion of carbon residues decreases with increasing fluence above 10^{17} ions/cm^2. Nevertheless, we are not able at this point to conclude on the origin of this decrease. Indeed, a potential transformation of the carbon residues into onion-like structures due to the irradiation effects, as it is the case under electron irradiation effects [1], can be proposed to explain it. On the other hand, this decrease could also be provided by a simple precipitation of all the implanted carbon species into carbon onions rather than in a residual form after a critical step which is not determined yet. Further characterizations of low-fluence implanted samples will be necessary to assess if this residual graphite can be considered as a simple contamination or as a significant contribution which plays an important role on the carbon onion formation.

In addition to the implantation fluence, the ion current density is another parameter which controls the onion optical properties, chiefly through temperature effects.

By increasing the current density, higher energy density per unit time is lost in the implanted samples. All the implanted carbon atoms stop inside the silver layer and the silica substrates constitute good thermal barreers. Therefore almost all the energy lost by the 120 keV carbon ions has to be dissipated in the silver layer. Thus, higher temperatures are realized in the implanted zone when the current density increased, and the optical response of the different carbon layers shows that this affects the quantity of graphitic residues. For instance, increasing the current density from 6 to 15 μA/cm^2 decreases the concentration of carbon residues by a factor of two (see table 1). This observation shows that the formation of the carbon residues is sensitive to the temperature of the substrate.

Finally, returning to the astrophysical aspect mentioned in the introduction, the optical results presented here do not bring direct new insights. Nevertheless, it is interesting to note that the redshift observed by Blanco *et al.* [15] and Wada *et al.* [14], when carbon materials were grown in various conditions of temperature and atmosphere, is very similar to what we observed. Our analysis shows that the aggregation of the carbon onions can contribute to this redshift. Furthermore it also shows that residual graphite plays an important role on the optical response. Thus, better comparison between astrophysical data and experimental results ask for large amount of isolated carbon onions. Concerning the carbon onions synthesized by ion-implantation, oxydation experiments have to be performed in order to separate the carbon onions but also to eliminate the residual component.

5 Conclusion

Carbon onions were produced by ion implantation into a silver thin film, and subsequently deposited on a silica substrate for analysis by optical transmission spectroscopy. Two absorption bands were found, at 0.23 and 0.265 μm, with relative intensities that depend on the synthesis conditions. Transmittance curves computed for idealized models of the carbon onion layer indicate that the 0.23-μm band is due to the carbon onions, which fill the layer with a volumic fraction $f = 0.6$. The absorption band at 0.265 μm is due to a small percentage of graphite residues in the voids between the carbon onions. The fraction of residues was shown to increase by decreasing either the ion current density or the fluence. At low fluences, the proportion of graphite residue is a few percents of the deposited carbon.

The authors acknowledge M.F. Denanot who performed the HRTEM analysis. Helpful discussion with Th. Henning and H. Mutschke are greatly acknowledged. This work has been partly funded by the interuniversity research project on reduced dimensionality systems (PAI P4/10) of the Belgian Office for Scientific, Cultural and Technical affairs. It has also benefited from a financial support from the "Actions intégrés franco-belges Tournesol" (Project N 98.034). L.H. was supported by the belgian FNRS.

References

1. D. Ugarte, Nature **359**, 707 (1992).
2. H. Terrones, M. Terrones, J. Phys. Chem. Solids **58**, 1789 (1997).
3. D. Ugarte, MRS Bull. **19**, 39 (1994).
4. L. Rapoport, Yu. Bilik, Y. Feldman, M. Homyonfer, S.R. Cohen, R. Tenne, Nature **387**, 791 (1997).
5. H.W. Kroto, Nature **359**, 670 (1992).
6. W.A. de Heer, D. Ugarte, Chem. Phys. Lett. **207**, 480 (1993).
7. D. Ugarte, Astroph. J. **443**, L85 (1995).
8. L. Henrard, Ph. Lambin, A.A. Lucas, Astrophys. J. **487**, 719 (1997).
9. L. Henrard, A.A. Lucas, Ph. Lambin, Astrophys. J. **406**, 92 (1993).
10. A.A. Lucas, L. Henrard, Ph. Lambin, Phys. Rev. B **49**, 2888 (1994).
11. E.L. Wright, Nature **336**, 227 (1988)
12. P. Apell, D. Ostling, G. Mukhapadyay, Solid State Comm. **87**, 219 (1993)
13. L. Henrard, P. Senet, Ph. Lambin, A.A. Lucas Synthetic Metals **77**, 27 (1996)
14. S. Wada, C. Kaito, S. Kimura, H. Ono, A.T. Tokunaga, Astron. Astrophys. **345**, 259 (1999).
15. A. Blanco, S. Fonti, V. Orifino, Astrophysical J. **448**, 339 (1995).
16. D. Ugarte, Europhys. Lett **22**, 45 (1993).
17. G. Lulli, A. Parisini, G. Mattei, Ultramicroscopy **60**, 187 (1995).
18. M.S. Zwanger, F. Banhart, Phil. Mag. B **72**, 149 (1995).
19. F. Banhart, T. Fullert, P. Redlich, P.M. Ajayan, Chem. Phys. Lett. **269**, 349 (1997).
20. T. Stöckli, J.M. Bonard, A. Chatelain, Z.L. Wand, P. Stadelmann, Phys. Rev. B **61**, 5751 (2000)
21. M. Kociak, L.Henrard, O. Stephan, K. Suenaga, C. Colliex, Phys. Rev. B **61**, 13936 (2000).
22. V.L. Kuznetsov, A.L. Chuvilin, Y.V. Butenko, I.Y. Mal'kov, V.M. Titov, Chem. Phys. Lett. **222**, 343 (1994).
23. T. Cabioc'h, M. Jaouen, M.F. Denanot, Europhys. Lett. **38**, 471 (1997).
24. T. Cabioc'h, E. Thune, M. Jaouen, Chem. Phys. Lett. **320**, 202 (2000).
25. W.T. Doyle, J. Appl. Phys. **49**, 795 (1978).
26. B. Michel, Th. Henning, C. Jäger, U. Kreibig, Carbon **37**, 391 (1999).
27. E. Tosati, F. Bassani, Nuovo Cimento **65**, 161 (1970).
28. This approximation is sufficent here, given the small percentage of residual graphite. More sophisticated models of randomly-oriented graphite exist, see reference [26].
29. C.F. Bohren, D.R. Huffman, *Absorption and scattering of light by small particles* (John Wiley and Sons, New York, 1983), p. 37.
30. B.T. Draine, H.M. Lee, Astrophys. J. **285**, 89 (1984); B.T. Draine, *Princeton Observatory Report* (Princeton, 1987).
31. T. Stöckli, J.M. Bonard, A. Chatelain, Z.L. Wang, P. Stadelmann, Phys. Rev. B **57**, 15599 (1998).
32. L. Henrard, F. Malengreau, P. Rudolf, K. Hevesi, R. Caudano, Ph. Lambin, Th. Cabioc'h, Phys. Rev. B **59**, 5832 (1999).